Study on Effects of Cooling Process on Mechanical and Tribological Properties of Melt-casting Copper-Steel Bimetallic Composites

Xiaoliang FANG, Yanguo YIN *, Shan HUANG, Ming XU, Jilin MIAO, Rongrong LI

School of Mechanical Engineering, Hefei University of Technology, No. 193 Tunxi Road, Hefei, Anhui, 230009, China

http://doi.org/10.5755/j02.ms.36016

Received 11 January 2024; accepted 11 April 2024

The ZCuPb15Sn5/1045 bimetallic composites were prepared by the melt-casting composite method. The mechanical and tribological properties of the copper-steel bimetallic composites under different cooling process conditions were studied. The results showed that with the acceleration of the cooling rate, the copper layer of the copper-steel bimetallic composite became harder, the grain became finer, and the distribution of the anti-friction element Pb became more uniform. Underwater cooling conditions, the shear strength increased, and the shear fracture gradually showed the tendency of tough and brittle fracture. The cooling process had a more significant influence on the tribological properties of the material. When the cooling rate was slow, the copper layer of the bimetallic composites had a high friction coefficient and relatively serious adhesive wear and oxidation wear. For the water cooling sample with a very fast cooling rate, the friction coefficient of the copper layer was low and the wear degree was relatively light.

Keywords: melt-casting composite method, copper-steel bimetallic composite, cooling process, shear, friction and wear.

1. INTRODUCTION

With the development of mechanical equipment, the requirements for the comprehensive performance of materials are also increasingly high, and the performance of parts made of single metal material is monotonous, which makes it challenging to meet the increasing high-performance requirements [1, 2].

Steel has the advantages of high strength and low cost, and lead bronze has the advantages of good thermal conductivity, abrasion resistance, and impact resistance. Therefore, the copper-steel bimetallic composites prepared with lead bronze as the composite layer and steel as the matrix layer have the excellent properties of both materials [3]. Copper-steel bimetallic composites have been widely used in sensors, motors, hydraulic pumps and other fields. Currently, the commonly used methods for preparing bimetallic composites include casting, spray molding, laser cladding, powder metallurgy, and melt-casting composite methods [4 – 10]. Many scholars at home and abroad have researched different preparation methods and molding processes to give full play to the performance advantages of copper-steel bimetallic composites.

Zhang et al. [11] prepared ZCuPb20Sn5/1045 bimetallic composites by casting method and by air-cooling method, they investigated the relationship between the microstructure and the tribological properties of the copper layer under oil-rich lubrication conditions, and the results showed that the Cu3P and δ (Cu31Sn8) phases in CuPb20Sn5 were distributed in the α-Cu to improve the wear resistance of the alloy. Althahban et al. [12] studied the effect of reinforcement (steel rod) preheating temperature on the mechanical properties of copper matrix composites, and the results showed that the best bond between the copper matrix and steel rod formed only in the composites prepared by preheating the steel rods with temperatures lower than the recrystallization temperature of steel (723 ℃). Yan et al. [13] studied the effect of size refinement and distribution of lubricating Pb phase on the wear rate in high-lead tin bronze by spray molding method, and the results showed that the Pb phase was finer and more dispersed in spray-formed bronze compared with traditional cast bronze, which reduced the wear rate. Wang et al. [14] prepared ZCuSn6Pb6Zn3/steel layered bimetallic composite specimens by powder metallurgy, and studied the interface microstructure, the results indicated that the bonding surface formed a powder metallurgy interface without a transition layer under the action of mechanochemistry when ZCuSn6Pb6Zn3 was sintered with steel, and the porosity was calculated about 15.414 %.

Compared with casting method, spray molding method, powder metallurgy method, and other bimetallic composite molding methods, the melt-casting composite method has more advantages in the preparation of high-performance bimetallic materials and parts because of its high interfacial bonding strength and more reliable bimetallic properties. However, the melt-casting temperature, holding time, cooling process, and other process conditions have certain effects on the interfacial bonding, microstructure uniformity, mechanical properties, and tribological properties of copper-steel bimetallic composites [12, 15, 16]. Among them, the cooling process is the key factor affecting the microstructure and performance of copper-steel bimetallic composites. At present, although there have been many studies on the effects of different process conditions or different compositions on the properties of melt-casting copper-steel bimetallic materials, the changes of microstructure, mechanical properties and tribological properties of copper layer of copper-steel

* Corresponding author. Tel.: +86-18919661022.
E-mail: *ygyin@hfut.edu.cn* (Y. Yin)

bimetallic composite materials by cooling process are still not systematically discussed. In this paper, the ZCuPb15Sn5/1045 bimetallic composite was prepared by melt-casting composite method. The effects of the cooling process on the microstructure, mechanics, and tribological properties of the copper-steel bimetallic composites were investigated, aiming to provide a theoretical basis and guidance for the preparation of high-performance copper-steel bimetallic composites.

2. MATERIALS AND METHODS

2.1. Experimental materials

ZCuPb15Sn5 copper alloy and 1045 steel were used to prepare copper-steel bimetallic composites. The chemical compositions of ZCuPb15Sn5 copper alloy and 1045 steel are shown in Table 1 and Table 2, respectively.

Table 1. Chemical composition of ZCuPb15Sn5 copper alloy (units/wt.%)

Cu	Sn	Pb	Fe	Sb	P	S
Bal.	5.11	15.36	0.12	0.17	0.03	0.03

The ZCuPb15Sn5 copper alloy was processed into φ42 mm × 6 mm round block and cleaned with anhydrous ethanol, and the 1045 steel was processed into a cylinder with a groove as shown in Fig. 1, the specific dimension was φ50 mm × 20 mm and the size of the groove was φ45 mm × 8 mm. The the 1045 steel sample was put into the ultrasonic cleaning machine and the steel surface was cleaned for 20 minutes with an aqueous cleaning agent and anhydrous ethanol in turn. Finally, anhydrous borax was used to clean the surface of 1045 steel matrix and enhance the fluidity of the copper alloy during the melt-casting process.

Table 2. Chemical composition of 1045 steel (units/wt.%)

Fe	C	Si	Mn	Cr	Ni	Cu
Bal.	0.44	0.21	0.63	0.14	0.12	0.09

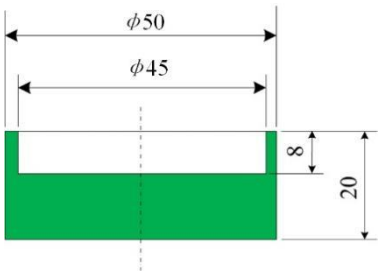

Fig. 1. Dimensions of 1045 steel substrate

2.2. Sample preparation and test method

Firstly, anhydrous borax and copper alloy blocks were put into the groove of a 1045 steel matrix in turn, the materials were melted and cast in the tubular resistance furnace of type SK-G08143, and nitrogen with a purity of more than 99.99 % was used as the protective atmosphere. The melting and casting temperature was set at 1100 ℃ to ensure that ZCuPb15Sn5 copper alloy was completely melted. The holding time was set to be 25 min. In the melt-casting process, the borax melted earlier than the copper alloy to form liquid because of its low melting point, and the specific gravity of borax is small, so when the copper alloy was completely melted, the borax would float to the surface of the molten copper alloy. After the end of insulation, three different cooling methods were used which were respectively cooling in the furnace (referred to as "furnace cooling"), cooling in the air (referred to as "air cooling") and cooling by immersion in water (referred to as "water cooling"). Water cooling was to immerse 1/3 of the steel matrix part of the bimetallic sample in water, which can achieve directional solidification of copper alloy, typical melting and casting defects such as shrinkage and porosity in the copper layer should be avoided [17]. Fig. 2 shows the schematic diagram of the bimetallic materials preparation process.

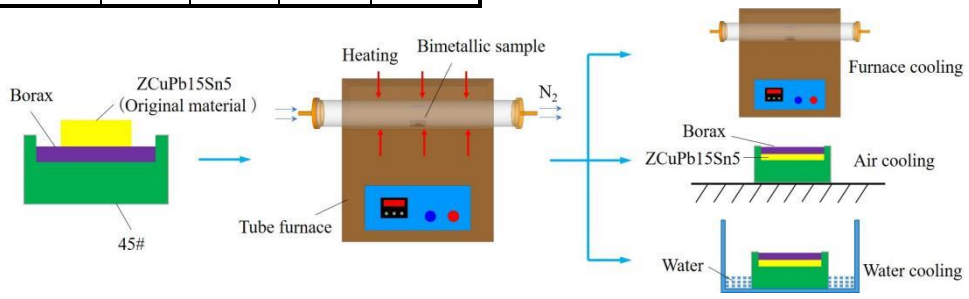

Fig. 2. Schematic diagram of the process of bimetallic composites preparation

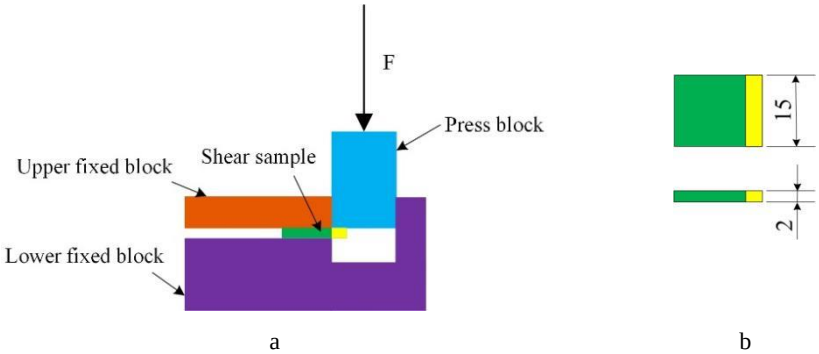

Fig. 3. a – schematic of the self-made shear fixture; b –the size of a shear sample

To eliminate the residual stress of the bimetallic sample prepared by water cooling and maintain the material's original microstructure, at low-temperature tempering treatment at 200 ℃ was adopted for 2 h. MR5000 optical metallographic microscope was used to observe the microstructure and morphology of copper-steel bimetallic composites. The self-designed shear fixture as shown in Fig. 3 a and the WDW-100M electronic universal testing machine were used to test the shear strength at room temperature, the size of the shear specimen was shown in Fig. 3 b. The shear fracture morphology and frictional wear morphology of copper-steel bimetallic composites were characterized by a Zeiss Sigma 300 scanning electron microscope (SEM) equipped with an energy dispersive X-ray spectrometer (EDS). The hardness of the bimetallic copper layer was measured by the HR-150A Rockwell hardness tester according to ASTM E18-22 standard.

The friction and wear test of the bimetallic copper layer was conducted using the MM-200 friction and wear testing machine, and the friction pair for the ring block contact form as shown in Fig. 4 a, the size of the bimetallic sample was 30 mm × 6 mm × 7 mm, and the specific specification was shown in Fig. 4 b. The lower specimen material was quenched 1045 steel with a hardness of 47 – 53 HRC, outer diameter of 40 mm, inner diameter of 15 mm and thickness of 10 mm. The dry friction method was used for the test, and the test time was 30 minutes. Under the constant rotational speed condition of 200 r/min, the load was set to 20 N, 35 N, and 50 N respectively. The friction coefficient of the friction pair was tested during the test, the wear volume was measured at the end of the test, and the three-dimensional morphology was measured with the Keyence VR-1000 three-dimensional profilometer on the worn-out samples.

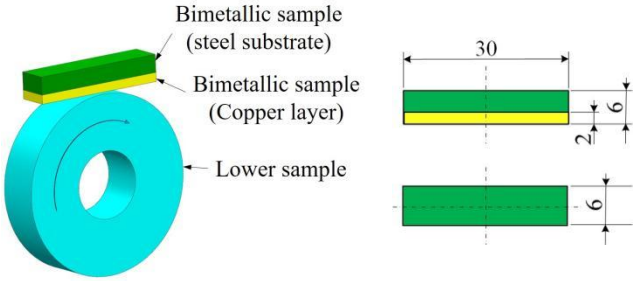

Fig. 4. a – schematic diagram of the friction test; b – size specification of bimetallic samples for friction test

3. RESULTS AND DISCUSSION

3.1. Microstructure and mechanical properties

Fig. 5 shows the cooling curves of bimetallic samples prepared under different cooling process conditions, from which it can be seen that from 1100 ℃ to 100 ℃, the time used in furnace cooling, air cooling, and water cooling are 274 min, 31 min, and 2 min, respectively.

There is a significant difference between the cooling speed of the three processes. The time used in furnace cooling is 8.8 times and 137 times longer than that in air cooling and water cooling, respectively.

Fig. 6 a, c and e show the metallographic structures of the copper layer of the bimetallic samples prepared under different cooling process conditions, it can be seen that the anti-friction element Pb exists in a monomorphic state.

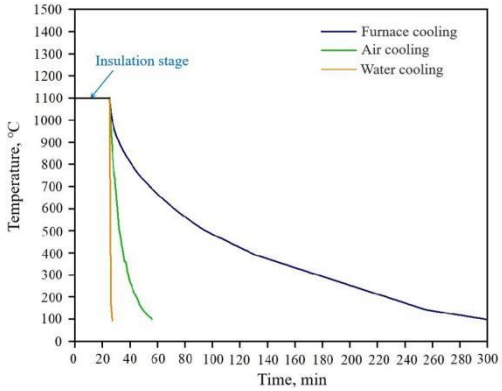

Fig. 5. Cooling curves for the preparation of bimetallic samples

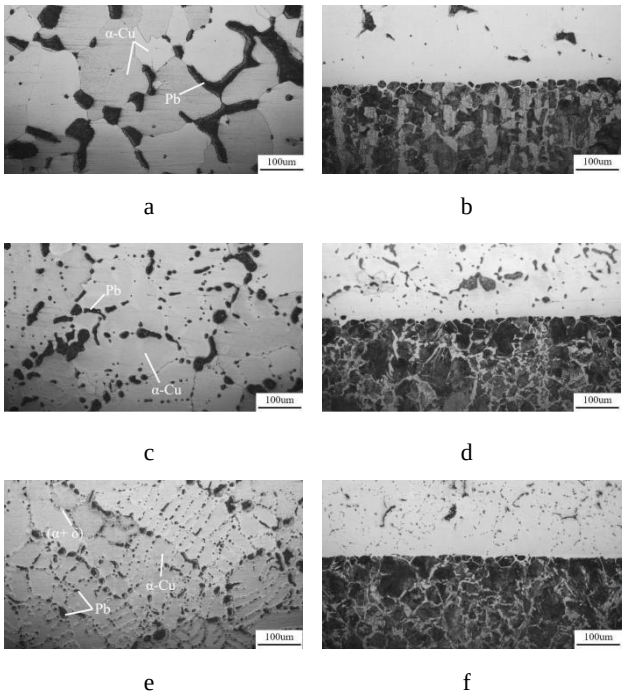

Fig. 6. Metallographic structures of the copper layer and interfaces of bimetallic samples prepared under different cooling conditions: a, b – furnace cooling; c, d – air cooling; e, f – water cooling

With the increase of the cooling rate, the grains of the copper layer are getting finer and finer. The Pb phases in the copper layer of the furnace cooling sample and air cooling sample are distributed in strips and blocks, and have a certain degree of segregation. The Pb phase of the furnace cooling sample has a large area of aggregation and segregation in local regions, while the aggregation and segregation of the Pb phase in the air cooling sample is slightly reduced. However, the Pb phase in the water cooling sample is distributed in spots and a few blocks, and the distribution is relatively uniform. The copper layer microstructure of the furnace cooling sample and air cooling sample is composed of Pb phase and α-Cu phase, and the Pb phase is distributed at the grain boundary of the α-Cu phase. For the water cooling sample, in addition to the Pb phase and α-Cu phase, there is also (α + δ) eutectoid phase in the copper layer microstructure, among which δ phase belongs

to the hard and brittle phase and is an intermetallic compound with the chemical composition of Cu31Sn8 [11]. Fig. 6 b, d, and f show the interface metallographic structures of the bimetallic samples prepared under different cooling process conditions, it can be seen that good metallurgical bondings are formed between the copper layer and the steel matrix, there are no shrinkage holes, cracks and other defects at the interfaces.

The thickness of the copper layer is retained by 3 mm to avoid the interference effect of the steel matrix on the hardness test of the copper layer. The hardness measurement results of the copper layer are shown in Fig. 7, it can be seen that the hardness of the copper layer of the bimetallic samples prepared by furnace cooling, air cooling, and water cooling is 65 HRF, 70 HRF, and 77 HRF, respectively.

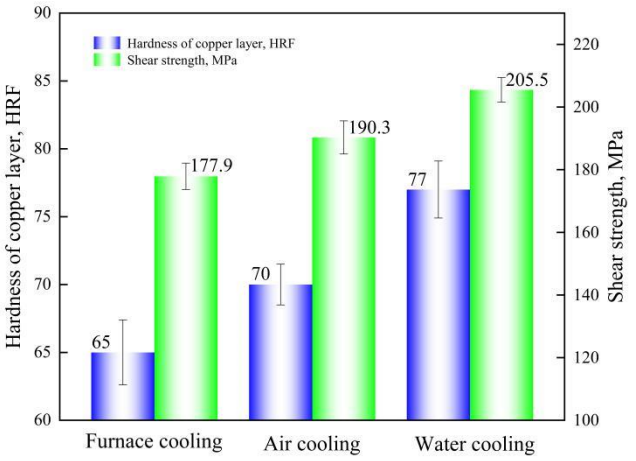

Fig. 7. The copper layer hardness and shear strength of bimetallic samples

The hardness of the copper layer is closely related to the cooling rate, the faster the cooling rate, the higher the hardness of the copper layer, which is mainly attributed to two aspects, on the one hand, the increase in the cooling rate promotes the grain refinement of the copper layer and the distribution of anti-friction element Pb is more uniform; on the other hand, the increase of cooling rate promotes the formation of hard and brittle δ phase.

Fig. 7 also shows the shear strength test results of ZCuPb15Sn5/1045 bimetallic composites prepared under different cooling process conditions. It can be seen that the order of shear strength is furnace cooling < air cooling < water cooling. The shear fracture mainly occurs on the copper side with lower strength, and the phenomenon of detachment from the copper-steel interface is not found. Fig. 8 shows the SEM morphology of the shear fracture, from which it can be seen that the shear fracture of the furnace cooling sample is a tearing ridge fracture formed by secondary cleavage, and there is a large plastic deformation between the two cleavage cracks which shows a ductile fracture. The shear fracture of the air cooling sample is a quasi-cleavage fracture composed of tearing ridges and a few dimples formed by secondary cleavage, and the fracture form is a ductile fracture. The shear fracture of the water cooling sample is a quasi-cleavage fracture composed of a few dimples and transgranular fractures, showing a mixture of tough-brittle fractures. The form of shear fracture of the bimetallic samples has a certain relationship with the metallographic structure of the bimetallic copper layer [18].

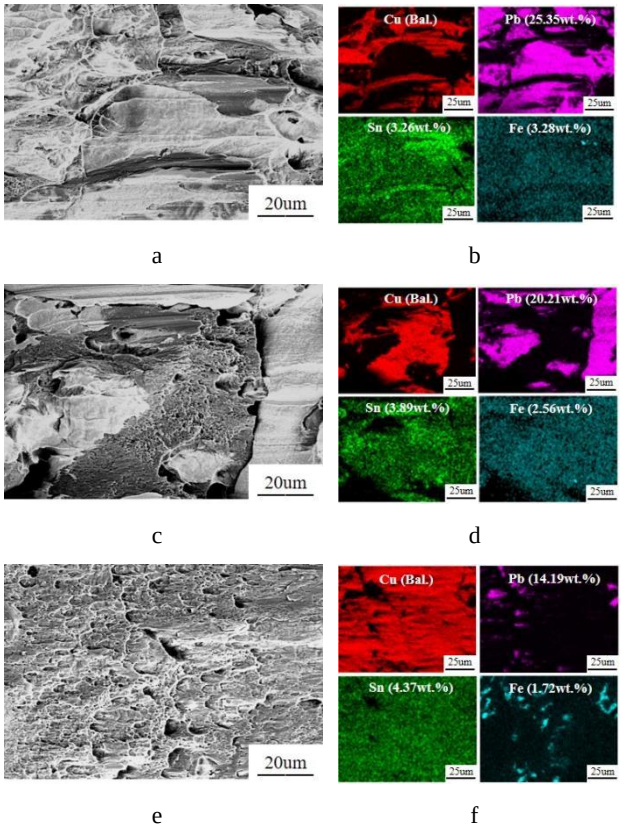

Fig. 8. SEM morphology and mapping scans of bimetallic samples prepared under different cooling conditions for shear fracture: a, b – furnace cooling; c, d – air cooling; e, f – water cooling

The copper layer of the furnace cooling and air cooling sample consists of Pb phase and α-Cu phase without hard and brittle phase, so its fracture form is ductile fracture, whereas there is a hard and brittle δ phase in the metallographic structure of the copper layer of the water cooling sample, which results in the form of tough-brittle mixed fracture [19].

Pb in the bimetallic copper layer tends to precipitate towards the interface during the cooling process, which leads to an increase in the Pb content at the interface, and Pb belongs to the soft element and exists in a monomorphic state, which is not conducive to the improvement of the shear strength of the bimetal. From the mapping scans of shear fracture in Fig. 8, it can be seen that the furnace cooling sample has a slow cooling rate and a lengthy precipitation and segregation time of Pb, resulting in a severe Pb segregation phenomenon at the interface of the sample, the distribution area of Pb is large, and the content of Pb at the shear fracture is as high as 25.35 wt.%. The cooling rate of the air cooling is higher than that of furnace cooling, which reduces the precipitation and segregation time of Pb, the segregation phenomenon of Pb at the interface is alleviated, the Pb content at the shear fracture is reduced to 20.21 wt.%, but the distribution area of Pb is still relatively large. The water cooling sample has a high-speed cooling rate, and Pb can not precipitate and segregate at the interface, therefore, the distribution of Pb at the interface is relatively uniform, and the Pb content at the shear fracture is only 14.19 wt.%, and the distribution area is small.

3.2. Friction and wear properties

3.2.1. Friction coefficient

The variation curves of the friction coefficient of the copper layers of the bimetallic samples prepared by furnace cooling, air cooling, and water cooling under different loads are shown in Fig. 9, the corresponding loads in Fig.9 a – c are 20 N, 35 N, and 50 N, respectively. At the beginning of the test, the friction coefficient of the copper layer of the bimetallic samples prepared by different cooling methods did not have a big difference because the surface state of the material and the test conditions were close to each other before the test. As the test proceeds, the friction coefficient of the copper layer of the furnace cooling sample appears to increase and has an obvious fluctuation phenomenon; the water cooling sample has the smallest friction coefficient, and the fluctuation is also tiny, and the friction coefficient curve is almost unchanged after the test of 10 min under different loading conditions, which reflects a better anti-friction and anti-adhesion performance; the friction coefficient of the air cooling sample is between furnace cooling sample and water cooling sample. This shows that the cooling rate greatly influences the friction coefficient of the copper layer of the bimetallic samples, and with the increase of the cooling rate, the friction coefficient of the copper layer of the bimetallic sample decreases and tends to stabilize gradually.

In the process of friction and wear, the Pb in the copper layer of the sample can form a lubricating film on the friction surface to reduce the contact and wear of the friction surface [20]. When the cooling rate is faster, the distribution of Pb is more uniform, and the lubrication film formed by Pb is more stable, which can continuously provide good lubrication and friction reduction. Therefore, the copper layer of the water cooling sample has a low friction coefficient and good stability. When the cooling rate is slow, Pb in the copper layer of the bimetallic sample prepared by furnace cooling and air cooling is prone to aggregate segregation and uneven distribution, which leads to the friction surface can not form a uniform lubrication film, resulting in a high and unstable friction coefficient. According to Fig. 9 d, it can be seen that the average friction coefficient of the copper layer of the water cooling sample under the loads of 20 N, 35 N, and 50 N are 0.035, 0.052, and 0.060, respectively, which tends to increase with the increase of the load. However, the overall friction coefficient is low, and the copper layer can quickly enter the stable friction and wear stage under the three loads. It indicates that elevating the cooling rate can improve the distribution state of Pb in the copper layer of the bimetallic sample, reduce the friction coefficient, and improve the material's friction reduction performance.

3.2.2. Wear volume and wear morphology

Fig. 10 shows the wear volume of the copper layer of the bimetallic samples prepared by furnace cooling, air cooling, and water cooling methods under different loads. It can be seen that the wear volume of the copper layer of the furnace cooling sample is relatively high, and the wear volume of the copper layer of the bimetallic sample decreases significantly with the increase in the cooling rate.

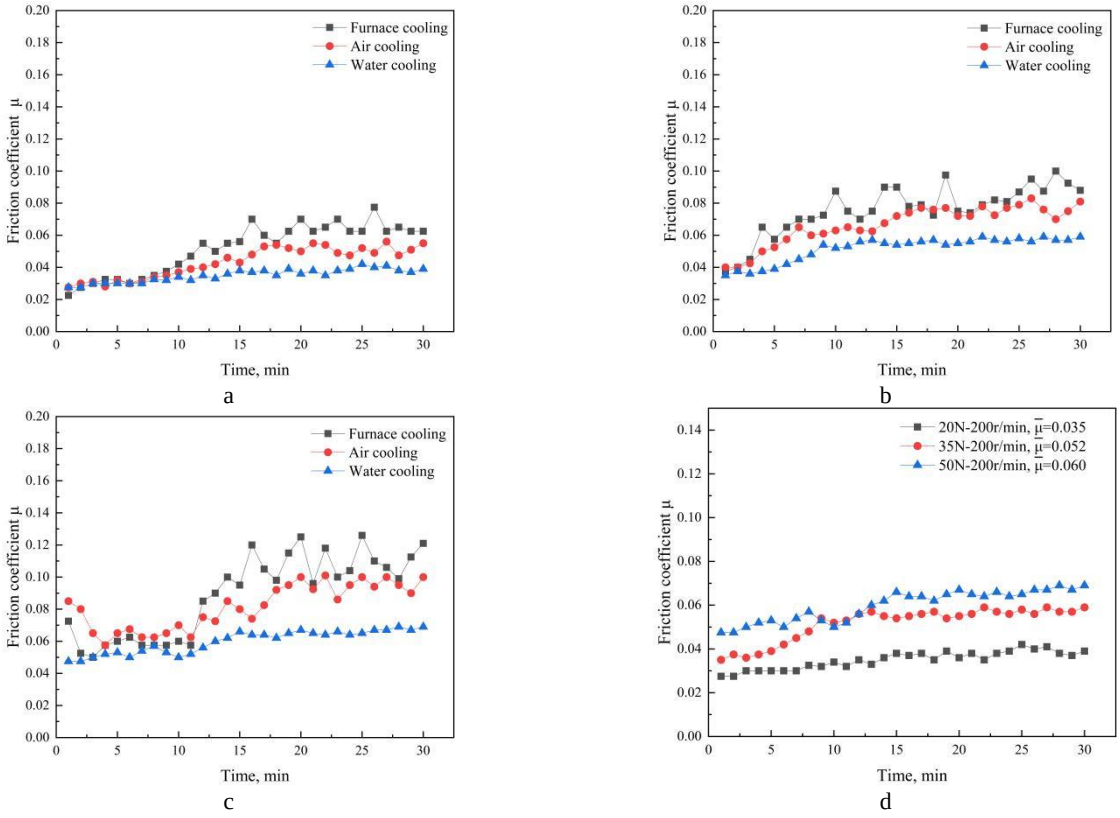

Fig. 9. Friction coefficient of copper layer of bimetallic samples under different load conditions: a – 20 N; b – 35 N; c – 50 N; d – water cooling

The wear volume of the copper layer of the bimetallic sample prepared under the same cooling condition increases gradually with the load, which corresponds to the changing trend of the friction coefficient.

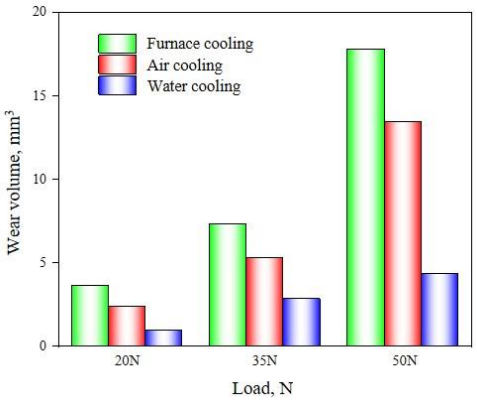

Fig. 10. Wear loss of bimetallic samples under different loads

The material's wear resistance can also be further explained by observing the surface wear morphology of the copper layer of the bimetallic samples. After the friction and wear test, the surface of the sample was cleaned by ultrasonic wave, and the surface morphology of the copper layer of the worn-out sample was measured and analyzed using a three-dimensional profilometer. Fig. 11 shows the 3D morphology and 2D cross-section profile of the copper layer of the sample under the load of 20 N. From this it can be seen that the abrasion cross sections all present a "U" shape and there are furrows on the wear surfaces [21], with the increase of the cooling rate, the wear surfaces of the copper layer of the samples all have different degrees of narrowing and shallowing, and the boundary areas of the wear surfaces become smaller, and the wear cross-section area of the samples prepared by the furnace cooling, air cooling and water cooling methods is 7743.7 μm^2, 6335.5 μm^2 and 4054.6 μm^2, respectively. It can be seen that the faster the cooling rate, the more uniform the Pb distribution in the copper layer of the bimetallic samples, and the higher the hardness, which not only improves the friction reduction performance of the copper layer of the bimetallic samples, but also improves its wear resistance.

3.2.3. Wear mechanism

Fig. 12 shows the SEM photographs and EDS analysis of the wear surfaces of the bimetallic samples prepared by furnace cooling, air cooling and water cooling methods after the friction wear test.

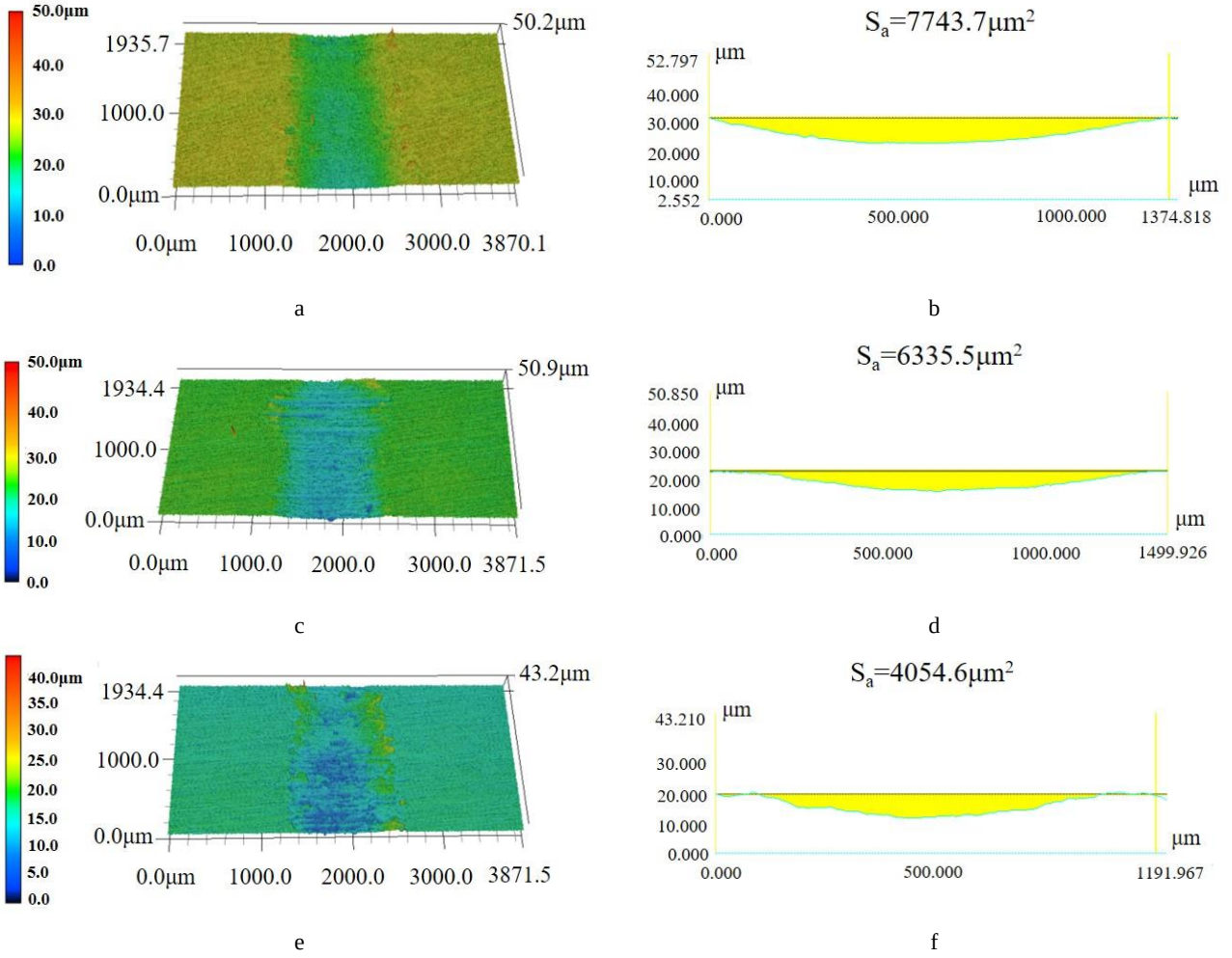

Fig. 11. The 3D morphology and 2D cross-section profile of bimetallic samples when the load is 20 N: a, b – furnace cooling sample; c, d – air cooling sample; e, f – water cooling sample

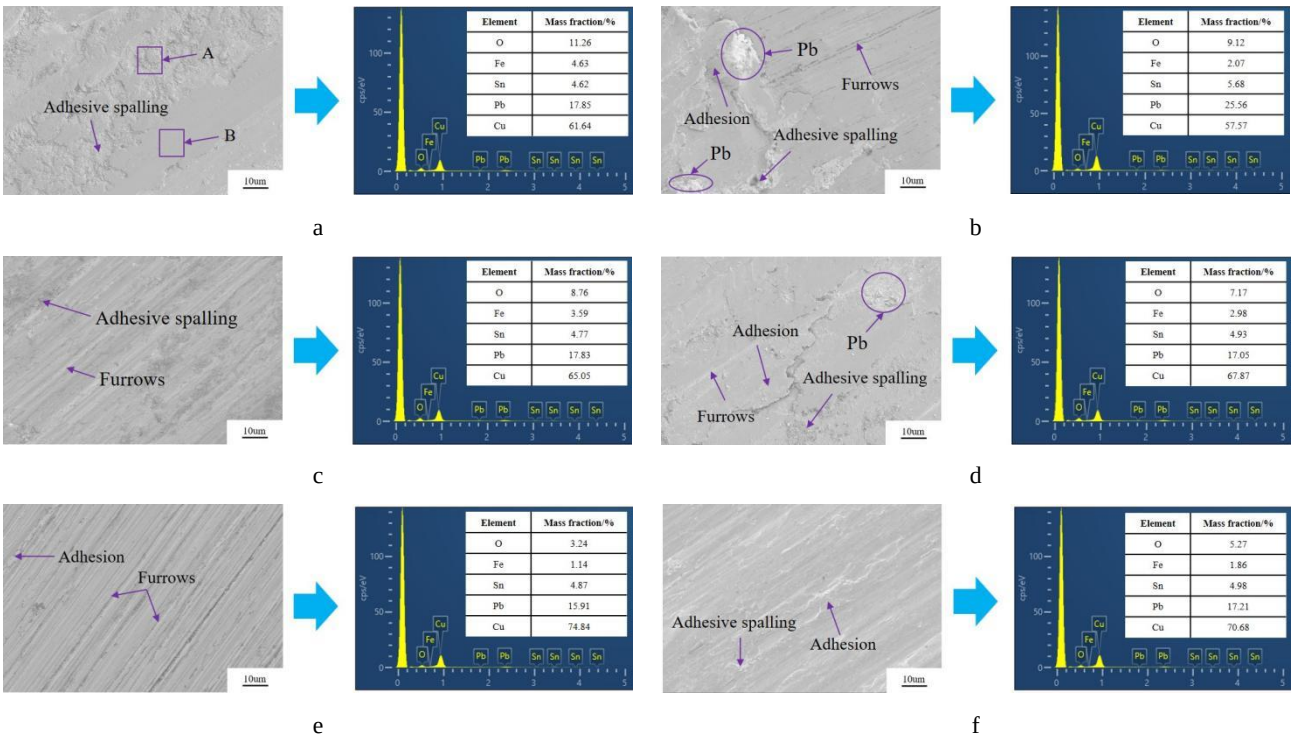

Fig. 12. Wear morphology and EDS results: a, b – furnace cooling sample; c, d – air cooling sample; e, f – water cooling sample

As shown in Fig. 12 a, the phenomenon of adhesion on the wear surface of the furnace cooling sample is more obvious, and adhesive spallings are found in local areas. According to the EDS detection, relatively large amounts of O (11.26 wt.%) and Fe (4.63 wt.%) are distributed on the wear surface. The chemical compositions of the adhesive region A and smooth region B were also tested, and the results are shown in Table 3. It can be found from the table that the content of O and Fe is high in the adhesive region A and low in the smooth region B.

Table 3. The chemical composition of local regions A and B in Fig. 12 a (units/wt.%)

Region	Cu	Pb	Sn	Fe	O
A	59.01	17.98	4.75	4.97	13.29
B	66.78	16.84	4.94	2.85	8.59

From Fig. 12 b, it can be seen that the copper layer of the furnace cooling sample has a few furrows and an obvious aggregation phenomenon of Pb locally, and the aggregated area of Pb is accompanied by crack extension, and the surface O and Fe content is relatively high (9.12 wt.% and 2.07 wt.%, respectively), which indicates that the surface of the copper layer has slight abrasive wear, but the adhesive wear and oxidation wear are relatively serious. It can be seen from Fig. 12 c and d that the wear surface of the air cooling sample also has furrows and a certain degree of adhesion and adhesive spalling. The contents of O/Fe on the wear surface shown in Fig. 12 c and d are 8.76 wt.%/3.59 wt.% and 7.17 wt.%/2.98 wt.%, respectively, which indicates that certain abrasive wear, adhesive wear and oxidative wear occur on the surface of the copper layer, but the wear degree is lower than that of the furnace cooling sample. As can be seen from Fig. 12 e and f, the wear surface of the water cooling sample is relatively smooth, and the wear is slight, there are a small number of furrows, adhesions, and adhesive spallings on the two wear surfaces, and the contents of O/Fe on the wear surface shown in Fig. 12 e and f are 3.24 wt.%/1.14 wt.% and 5.27 wt.%/1.86 wt.%, respectively, indicating that the water cooling sample has abrasive wear, adhesive wear and slight oxidative wear, but the wear degree was the lowest among the three types of samples.

The EDS results in Fig. 12 a and b also show that the Pb content of the two wear surfaces of the furnace cooling sample is 17.85 wt.% and 25.56 wt.%, respectively, and obvious Pb aggregation and segregation phenomenon can also be observed on the SEM photograph in Fig. 12 b, which is caused by the original distribution of Pb in the furnace cooling sample. Although the Pb content is generally high, due to Pb's aggregation and uneven distribution, adhesive wear and oxidative wear are more serious. The EDS results in Fig. 12 c and d show that the Pb content on the two wear surfaces of the air cooling sample is 17.83 wt.% and 17.05 wt.%, respectively, and there is a small amount of accumulation and segregation of Pb locally, which is lower than that of the air cooling sample. The soft phase Pb with a low melting point plays a good anti-friction and anti-adhesion role in the process of friction and wear, so the degree of adhesive wear and oxidative wear is lower than that of the furnace cooling sample. Furthermore, the Pb content of the two wear surfaces of the water cooling sample is 15.91 wt.% and 17.21 wt.%, respectively, and there is no obvious Pb aggregation and segregation phenomenon, the anti-friction and anti-adhesion effect of Pb is more obvious.

4. CONCLUSIONS

1. The faster the cooling rate, the higher the hardness and the finer the grain of the copper layer of the copper-steel bimetallic composites, and the more uniform the distribution of the Pb phase. The copper layer of the furnace cooling sample and air cooling sample is composed of α-Cu and Pb phase, and that of the water cooling sample consists of α-Cu, Pb phase, and δ-hard brittle phase.
2. The precipitation and segregation of Pb at the interface of ZCuPb15Sn5/1045 bimetallic composites are related to the cooling rate. The faster the cooling rate, the less precipitation and segregation of the Pb phase and the higher the shear strength. When the cooling method is furnace cooling and air cooling, the shear fracture form is a ductile fracture. When the water cooling method is used, the shear fracture form is a tough-brittle mixed fracture due to the generation of δ hard brittle phase.
3. The faster the cooling rate, the more uniform the distribution of the Pb phase in the copper layer of the bimetallic composites, the lower the friction coefficient, and the smaller the wear loss. The bimetallic samples prepared under different cooling process conditions all have a certain degree of abrasive wear, adhesive wear and oxidative wear, but the wear degree varies greatly.

Acknowledgments

This research was supported by the National Natural Science Foundation of China (Grant No.51575151 and No.51775158).

REFERENCES

1. **Guo, Y.Y., Wu, X.W., Ren, G.X., Liu, Z.P., Yuan, R.D., Yang, X., Dong, P.** Microstructure and Properties of Copper-steel Bimetallic Sheets Prepared by Friction Stir Additive Manufacturing *Journal of Manufacturing Processes* 82 2022: pp. 689 – 699. https://doi.org/10.1016/j.jmapro.2022.08.022
2. **Sun, Y.F., Fujii, H., Takaki, N., Okitsu, Y.** Microstructure and Mechanical Properties of Dissimilar Al Alloy/steel Joints Prepared by a Flat Spot Friction Stir Welding Technique *Materials & Design* 47 2013: pp. 350 – 357. https://doi.org/10.1016/j.matdes.2012.12.007
3. **Tan, C.L., Zhou, K.S., Ma, W.Y., Min, L.** Interfacial Characteristic and Mechanical Performance of Maraging Steel-Copper Functional Bimetal Produced by Selective Laser Melting Based Hybrid Manufacture *Materials & Design* 155 2018: pp. 77 – 85. https://doi.org/10.1016/j.matdes.2018.05.064
4. **Onuike, B., Heer, B., Bandyopadhyay, A.** Additive Manufacturing of Inconel 718-Copper Alloy Bimetallic Structure Using Laser Engineered Net Shaping (LENS^{TM}) *Additive Manufacturing* 21 2018: pp. 133 – 140. https://doi.org/10.1016/j.addma.2018.02.007
5. **Ghosh, M., Chatterjee, S.** Effect of Interface Microstructure on the Bond Strength of the Diffusion Welded Joints Between Titanium and Stainless Steel *Materials Characterization* 54 (4 – 5) 2005: pp. 327 – 337. https://doi.org/10.1016/j.matchar.2004.12.007
6. **Kostornov, A.G., Fushchich, O.I., Chevichelova, T.M.** Structurization in Sintering of Antifriction Powder Materials Based on Iron-copper Alloys *Powder Metallurgy and Metal Ceramics* 46 (11) 2007: pp. 589 – 594. https://doi.org/10.1007/s11106-007-0089-2
7. **Hajjari, E., Divandari, M., Razavi, S.H., Emami, S.M., Homma, T., Kamado, S.** Dissimilar Joining of Al/Mg Light Metals by Compound Casting Process *Journal of Materials Science* 46 2011: pp. 6491 – 6499. https://doi.org/10.1007/s10853-011-5595-4
8. **Song, D.B., Wang, T., Jiang, S.Y., Zhang, L.** Microstructure and Mechanical Properties of Copper–steel Laminated and Sandwich Joints Prepared by Electron Beam Welding *Journal of Materials Engineering and Performance* 29 2020: pp. 4251 – 4259. https://doi.org/10.1007/s11665-020-04960-1
9. **Zhang, H., Jiao, K.X., Zhang, J.L., Liu, J.P.** Comparisons of the Microstructures and Micro-mechanical Properties of Copper/steel Explosive-bonded Wave Interfaces *Materials Science and Engineering A* 756 2019: pp. 430 – 441. https://doi.org/10.1016/j.msea.2019.04.064
10. **Zhang, Y.B., Liu, J.M., Fu, Y., Jie, J.C., Lu, Y.P., Guo, Q.T., Wang, T.M., Li, T.J.** Microstructure and Fabrication of Cu-Pb-Sn/Q235 Laminated Composite by Semi-solid Rolling *Metals* 8 (9) 2018: pp. 722. https://doi.org/10.3390/met8090722
11. **Zhang, G.W., Kang, Y.Y., Liu, Y.J., Wang, Z.J., Xu, H.** Study on Tribology of Liquid-solid Formed CuPb20Sn5/Carbon Steel Bimetal *Materials Research Express* 9 (2) 2022: pp. 026502. https://doi.org/10.1088/2053-1591/ac4c17
12. **Althahban, S., Jazaa, Y., Bafakeeh, O., Alomari, A.S., Sallam, H.E.M., Atta, M.** The Effect of Reinforcement Preheating Temperatures on Tribological Behavior of Advanced Quranic Metal-matrix Composites (QMMC) *Materials* 15 (2) 2022: pp. 659. https://doi.org/10.3390/ma1502065
13. **Yan, P.F., Wang, D.P., Yan, B., Mo, F.** Effect of Size Refinement and Distribution of the Lubricating Lead Phases in the Spray Forming High-leaded Tin Bronze on Wear Rates *Modern Physics Letters B* 27 (19) 2013: pp. 1341019. https://doi.org/10.1142/S0217984913410194
14. **Wang, J.M., Duan, L.T., Wang, B.A.** Interface Microstructure and Bonding Energy of Layered Bimetallic ZCuSn6Pb6Zn3/steel Coupling with Temperature and Pressure *Tribology International* 155 2021: pp. 106754. https://doi.org/10.1016/j.triboint.2020.106754
15. **Kang, Y.Y., Zhang, G.W., Wang, Z.J., Xu, H., Wan, A.** Effect of Two-stage Cooling on the Microstructure and Tribological Properties of Steel–copper Bimetals *Materials* 15 (2) 2022: pp. 492. https://doi.org/10.3390/ma15020492
16. **D'Andrea, D., Epasto, G., Bonanno, A., Guglielmino, E., Benazzi, G.** Failure Analysis of Anti-friction Coating for Cylinder Blocks in Axial Piston Pumps *Engineering Failure Analysis* 104 2019: pp. 126 – 138. https://doi.org/10.1016/j.engfailanal.2019.05.041
17. **Zhang, X.Y., Zhang, T., Tan, C.W., Su, J.H., Chen, B., Song, X.G.** Improving the Interfacial Bonding Strength and Suppressing Shrinkage Porosity of 6061Al/GFRTP Hot-pressing Joints Via Interfacial Modification *Journal of Manufacturing Processes* 102 2023: pp. 490 – 500. https://doi.org/10.1016/J.JMAPRO.2023.07.072
18. **He, B., Li, J., Cheng, X., Wang, H.M.** Brittle Fracture Behavior of a Laser Additive Manufactured Near-β Titanium

Alloy after Low Temperature Aging *Materials Science and Engineering A* 699 2017: pp. 229 – 238. https://doi.org/10.1016/j.msea.2017.05.050

19. **Seo, K.W., Kim, Y.J., Hwang, J.H., Kim, K.S.** Finite Element Simulation Method for Combined Ductile-brittle Fracture of Small Punch Test in Hydrogen *Engineering Fracture Mechanics* 289 2023: pp. 109489. https://doi.org/10.1016/j.engfracmech.2023.109489
20. **Han, C.H., Li, G.L., Ma, G.Z., Shi, J.D., Wei, A.B., Li, Z., Yong, Q.S.E., Wang, H.D., Wang, H.P.** Research on Atomic Oxygen Erosion Influence of Structural Damage and Tribological Properties of Mo/MoS2-Pb-PbS Thin Film *Materials* 15 (5) 2022: pp. 1851. https://doi.org/10.3390/ma15051851
21. **He, T.T., Song, G.A., Shao, R.N., Du, S.M., Zhang, Y.Z.** Sliding Friction and Wear Properties of GCr15 Steel under Different Lubrication Conditions *Journal of Materials Engineering and Performance* 31 (9) 2022: pp. 7653 – 7661. https://doi.org/10.1007/S11665-022-06782-9